Analysing Gas-Liquid Flow in PEM Electrolyser Micro-Channels Using a Micro-Porous Ceramic as Gas Permeable Wall

Lafmejani, Saeed Sadeghi; Olesen, Anders Christian; Al Shakhshir, Saher; Kær, Søren Knudsen

Published in:
ECS Transactions

DOI (link to publication from Publisher):
10.1149/08008.1107ecst

Publication date:
2017

Document Version
Early version, also known as pre-print

Analysing Gas-Liquid Flow in PEM Electrolyser Micro-Channels using a Micro-Porous Ceramic as Gas Permeable wall

S. S. Lafmejani, A. C. Olesen, S. Al Shakhshir, S. K. Kær

Energy Technology Department, Aalborg University, 9000 Aalborg, Denmark.

Gas-liquid flow in micro-channels of a polymer electrolyte membrane water electrolysis cell (PEMEC) is studied ex-situ experimentally. In this study, the anode transport layer and micro-channels of an interdigitated flow field are visualised. A micro-porous ceramic is used for uniformly distributing gas. Different gas-liquid flow regimes like bubbly flow, Taylor flow and annular flow are noticed. These gas-liquid flow regimes are found to be dependent on current density and water stoichiometry. Furthermore, wall dry out in Taylor and annular flow regimes is noticed. This phenomenon is due to the channel cross-section aspect ratio and gas-liquid wall contact angle. This study gives knowledge about the flow plate design for high mass transport and heat transfer rates to and from the transport layer.

Introduction

The rise in the global temperature in recent years has increased the need to utilise more renewable energy sources. It is agreed that the main cause of the recent global warming is greenhouse gases (1). Therefore, using more renewable energy sources like wind and solar is necessary. Unlike traditional power plants like thermal and hydro power plants, wind farms and solar plants do not follow the consumers' energy demand. They follow climate conditions like the wind speed and the sunshine. To adapt to such conditions, there is a need for some sort of energy storage to even out fluctuations. Renewable energy can be stored electrochemically in large batteries, mechanically by flywheels, through high elevation water pumping, air compressing, electrochemically converting to hydrogen gas, etc (2). Between these options, hydrogen has a special importance. With the transition from fossil to sustainable resources, the demand for a flexible energy carrier like hydrogen is increasing. It can be regarded as an alternative energy carrier that stores chemical energy. It can be used in different applications from combustion based power generation sources like thermal engines to electrochemical-based power generation sources like fuel cells in hydrogen vehicles. It has also many applications in chemical plants (2).

PEMEC plays a key role in the future grid stabilisation by absorbing surplus of electricity. PEMEC has a fast response time, and can produce high pressure and high purity hydrogen from water and fluctuating renewable electricity from wind and solar farms.

At present, PEMEC is costly. Its working environment is highly corrosive; therefore, metals like titanium and platinum are required to survive that environment. Many research studies have introduced alternative materials to reduce PEMEC cost. On the other hand,

the price could be reduced by increasing hydrogen production from these cells. In other words by increasing the cell current density at the same voltage. At present, conventional cells are working at 1 - 2 A/cm^2. The current density should be increased to more than 10 A/cm^2 as a long term target to reduce the price and improve applicability (3). Nevertheless, increasing cell current density needs increasing heat removal and mass transport rates. At high current density, water flow rate, flow plate design and the transport layer characteristics become very crucial. Non-optimum design of these components results in maldistribution of water in the channels and the transport layers, which can lead eventually to hot membrane spots and dry outs resulting in cell performance degradation. In this context, Fouda-Onana et al. (4) found that high temperature degrades the membrane more than the current density.

The gas-liquid flow in the anode transport layer has a significant impact on cell performance. The transport layer transports oxygen and water depending on the specific transport rate. This rate can reach its limit at high current densities. Ito et al. (5) investigated the influence of pore structural properties of current distributors on the performance of PEMEC. The smaller pore sizes give a better contact between current distributor and the electrode that result in reduction in activation over potential. They revealed that "produced gas bubbles hinder the water supply to the electrode, when the mean pore diameter of the anode transport layer is less than about 50 μm, the effect of the decrease in water supply on the membrane resistance is limited" (5).

Flow plates are one of the key components in PEMEC cell stacks for hydrogen production. Flow plates must be properly designed to distribute reactant (water) evenly. The uniform water distribution needs an optimum design of the flow plates. Nie et al. (6) numerically and experimentally studied fluid flow in parallel channels of an electrolysis cell. They concluded that, liquid flow rate in the channels are parabolic. It means the middle channels have much lower water flow than the side channels. This difference makes a high temperature zone at the centre and especially close to the exit of the flow plate channels.

Yang et al. (7) experimentally investigated gas-liquid flow in a direct methanol fuel cell (DMFC), single serpentine and parallel flow fields with different size by constructing transparent cells. They concluded that a serpentine flow field results in a better performance. They showed blockages of gas in the parallel flow plate. The gas blockage was never noticed in serpentine flow plate. Because the sweeping rate of the gas bubbles is lower in the parallel flow field than the serpentine one. Also around 50 % open ratio (channel to active area) led to the best cell performance at moderate and high liquid (methanol) flow rates; while either larger or smaller open ratios resulted in cell performance degradation. Zhao et al. (8) in their review paper compared several flow fields like serpentine and parallel. They also concluded that serpentine flow field shows higher and more stable performance.

Wood et al. (9) analysed interdigitated and parallel channel flow plates in PEMFCs. They demonstrated a higher performance of interdigitated flow plate channel. It had higher voltage and higher power density. They showed that it improves the power increase limitation due to mass transport to the GDL. Even though there are many studies on different flow field designs, it appears that there are no experimental literature on the interdigitated flow plate performance in PEMECs.

CFD modelling can significantly improve our knowledge on gas-liquid flow and temperature distribution in PEMEC flow plate and transport layer. Olesen et al. (10) CFD modelled multiphase flow in a circular-planar, interdigitated anode flow field of a high pressure PEMEC. They investigated in their study the effect of flow plate design on temperature distribution. They recommended water stoichiometry (WST) higher than 350 to avoid that the temperature difference between maximum temperature and mean temperature exceeds 4K. Lafmejani et al. (11) numerically investigated gas-liquid flow in a long interdigitated micro-channel. They showed different gas-liquid flow regimes like bubbly flow and Taylor flow. Their result showed the importance of gas-liquid wall contact angle and the channel cross sectional geometry on avoiding flow plate channel dryness. They concluded that either a channel cross section closer to the ratio of one or adding more hydrophilicity to the wall reduces wall dryness.

CFD simulations can be validated using experimental findings. There are a few experimental studies on two-phase flow in the context of PEMEC. Selamet et al. (12) used simultaneous neutron radiography and optical image to visualise two-phase flow in anode and cathode sides of an electrolysis cell. They analysed influence of operating parameters such as current density, temperature and water flow rate on the two-phase flow distribution. They detected higher water accumulation in the cathode chamber at higher current density. Dedigama et al. (13) used electrochemical impedance spectroscopy (EIS) on a transparent PEMEC cell to provide information about individual contributions to the total impedance (losses) of an electrochemical system such as electrolyte conductivity and electrode processes. They also analysed localised current density mapping and flow visualisation in PEMEC. Their study revealed that as the gas-liquid flow transforms from bubbly to Taylor flow towards the end of the channel, current density also increases (14). It is concluded that this is due to the change in the gas-liquid flow regime. Meanwhile, the authors of this paper also suggest that it might be due to an increase in water temperature from inlet to outlet that resulted in increase in current density.

PEMEC is a complicated electrochemical device. Therefore, it makes more sense to analyse and study the involved processes separately to understand the effects of each of the governing parameters. In this context, removing the complexity of electrochemistry will improve the control of the influencing parameters. Yang et al. (15) characterised air-water flow in a mini channel with hydraulic diameter of 5 mm, using a gas permeable side wall that was made of a long porous lime wood block. The aim of the experimental setup was to show which two-phase flow regimes are encountered in direct feed methanol fuel cells. They visualised flow patterns in vertical and horizontal flows and identified two-phase flow regimes such as bubbly flow, plug flow, Taylor flow and annular flow. They showed that in the vertical flow, a single layer of gas bubble adjacent to the permeable sidewall is formed. Their conclusion showed that, the annular flow should be avoided as it may deteriorate the direct methanol fuel cell performance.

Lafmejani et al. (16) presented an experimental test case that consisted of two channels, one for air and the other for air-water flow. They noticed a non-uniform bubble growth; from the top and the bottom of the Ti-felt porous transport layer. This was due to the absence of a high resistance in the air flow. In this study, the previous experimental case is modified with a micro-porous ceramic that is added behind the Ti-felt. The micro-porous ceramic has a higher air flow resistance. The air flow resistance is much higher than the

water column pressure, therefore the water shouldn't block the air flow through the transport layer.

Experimental Equipment

Test cell

The vertical test cell is illustrated in Figure 1. To investigate the anode side of a PEMEC ex-situ, a test cell was constructed that consisted of a flow plate with micro-channels, Teflon gasket, porous transport layer (PTL) and a micro-porous ceramic plate placed in a Plexiglas plate. The micro-channel plate is made of Plexiglas with interdigitated channels. The active area covered by three channels, two inlet channels allowing water to transport into the active area and an outlet channel that directs gas-liquid flow out of the test section. The active area is 11 mm wide and 94 mm long. Water is supplied from the bottom of the channel and the air-water flows out from the top of the channel. The Teflon gasket thickness is 320 µm. PTL is a Ti-felt with 350 µm thickness. The micro-porous ceramic plate is 6 mm thick. It is a porous ceramic plate with channels inside to distribute air from the bottom of the air channel throughout the whole ceramic. Both ceramic and Ti-felt are hard materials with coarse surfaces. A carbon paper was added in between the Ti-felt and the ceramic to increase the interfacial contact. The soft carbon paper fills the gaps between them. The three micro channels have 1mm width, 94mm length and 0.5mm depth. There are two incoming channels that guide water from the bottom of the channels and one outgoing channel that guides out the gas-liquid flow from the top of the channel.

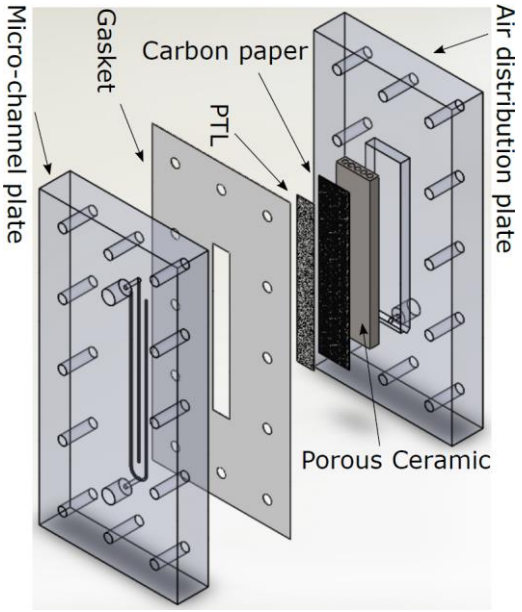

Figure 1: 3D view of the constructed transparent testing cell parts. The three channels in the micro-channel plate are arranged interdigited.

Test set-up

Experiments were carried out in the test set-up that is schematically shown in Figure 2. A centrifugal aquarium pump was used to pump DI-Water to the test section, while the laboratory air was fed into the microporous ceramic.

Flow visualisation

An AOS camera was employed to visualise flow pattern in the test section with a frame rate of 500 fps at a resolution of 1280 by 1024 pixels. An "AF Micro-Nikkor 60mm f/2.8D" was used to capture about 3 cm of the channel length. Two LED lights with 10 watts power were installed on each side of the test cell (or camera) to meet the required lightning for capturing images. As shown in Figure 2 (a), light from both sides of the camera illuminates the gas-liquid flow within the channel. The photos were processed using a MATLAB code to remove the photo background and to emphasize bubble borders.

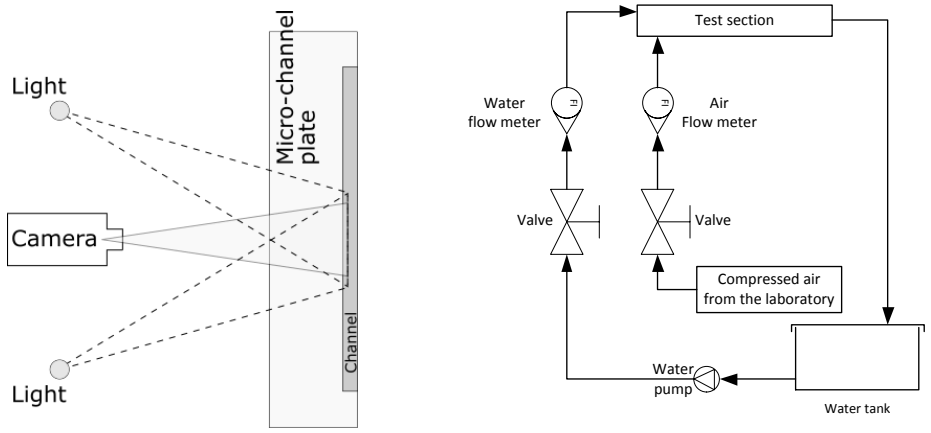

(a) (b)

Figure 2: (a) The visualisation system setup, (b) Schematic of the test set-up.

Results and discussion

Figure 3 shows bubbles in the middle section of the outlet channel. The photos were taken from the middle of the test cell. The view area is 3 cm long. The cell is operated under a fixed water stoichiometry of 100, with different air flow rates equivalent to current densities of 1 to 8 A/cm^2. Long Taylor bubbles with slightly different sizes can be distinguished in (a). There are also a few small Taylor bubbles in between the long ones. The same behaviour is noticed in (b) and (c). Furthermore, the figures reveal that a thin film of water is separating the Taylor bubbles from each other. A column of small Taylor bubbles covers the channel length in (d). At the bottom, there exists bubbly flow, but at the top, small Taylor bubbles are seen. In the figure from (a) to (d), both gas and liquid flow rates are increased.

Since each of the gas-liquid flow regime has its specific heat transfer properties, the desired gas-liquid flow regime can be controlled by adjusting the water stoichiometry. By mapping gas-liquid flow regimes in electrolyser micro-channels at several current densities and water stoichiometries, the gas-liquid regime will get controllable.

Figure 4 shows a qualitative gas-liquid flow map based upon Figure 3. It shows that by increasing both the gas and liquid flow rate, the flow regime from the Taylor region enters the bubbly region. Lafmejani et al. (11) concluded in their simulation that a uniform distribution of bubble shapes and sizes along the channel length without a large gaps in between the bubbles would result in a more uniform water flow in the PTL.

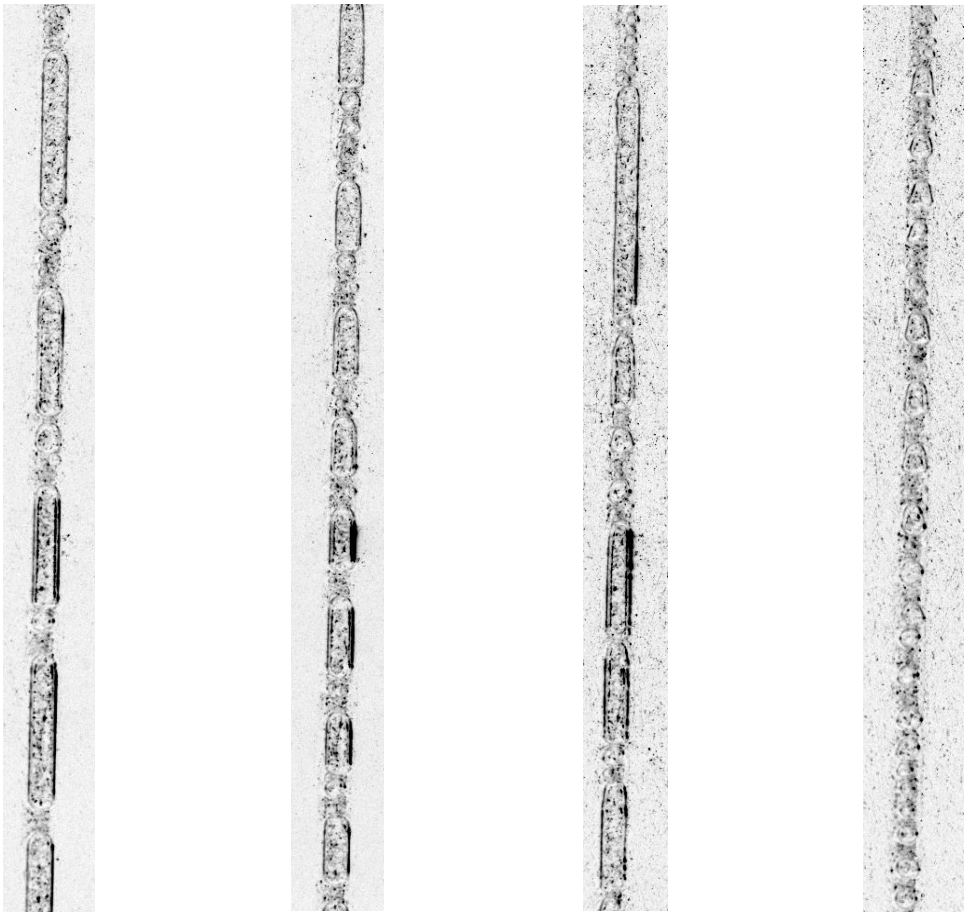

(a) I = 1 A/cm^2, WST=100 (b) I = 2 A/cm^2, WST=100 (c) I = 4 A/cm^2, WST=100 (d) I = 8 A/cm^2, WST=100

Figure 3: Gas-liquid flow in the middle section of the channel, at fixed water stoichiometry of 100 and different gas flow rate equivalent 1 to 4 (a - d) demonstrating different current densities.

Figure 5 shows different bubble types at different operating conditions in the outgoing channel. Photos are taken from 3 cm height at the middle of the test cell. The bubbles are captured at fixed air flow rate equivalent to current density of 4 A/cm^2. They have different water flow rates equivalent to water stoichiometries from 25 to 200.

The gas-liquid flow regime is annular bubble at water stoichiometry of 25 as seen in Figure 5(a). By increasing the water stoichiometry to 50, the cylindrical border of the annular bubble becomes wavy (b). It is an indicator of the tendency of the annular bubble border to split into parts. It is seen in (c) that the annular bubble splits into Taylor bubbles by increasing the water stoichiometry to 100. There are several Taylor bubbles that at some point merge and build larger Taylor bubbles at the top of the channel. At a water stoichiometry of 200, only bubbly flow is seen in (d), which is not clear in the picture. In

general, at a fixed current density, by increasing the water stoichiometry, bubbles split into slices and the bubbly flow changes regime from annular to Taylor bubbles to bubbly flow.

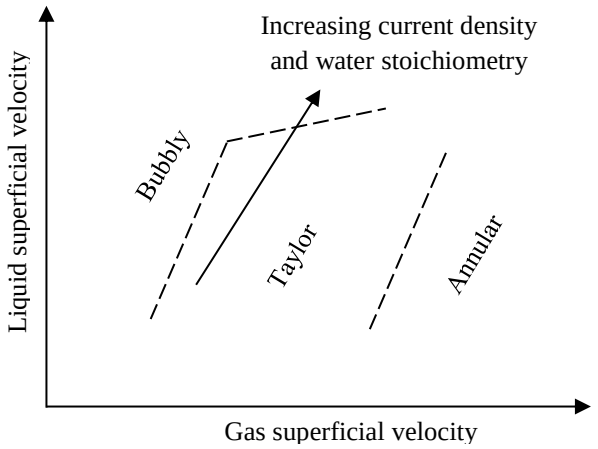

Figure 4: Qualitative gas-liquid flow map depicted from the experimental captured images.

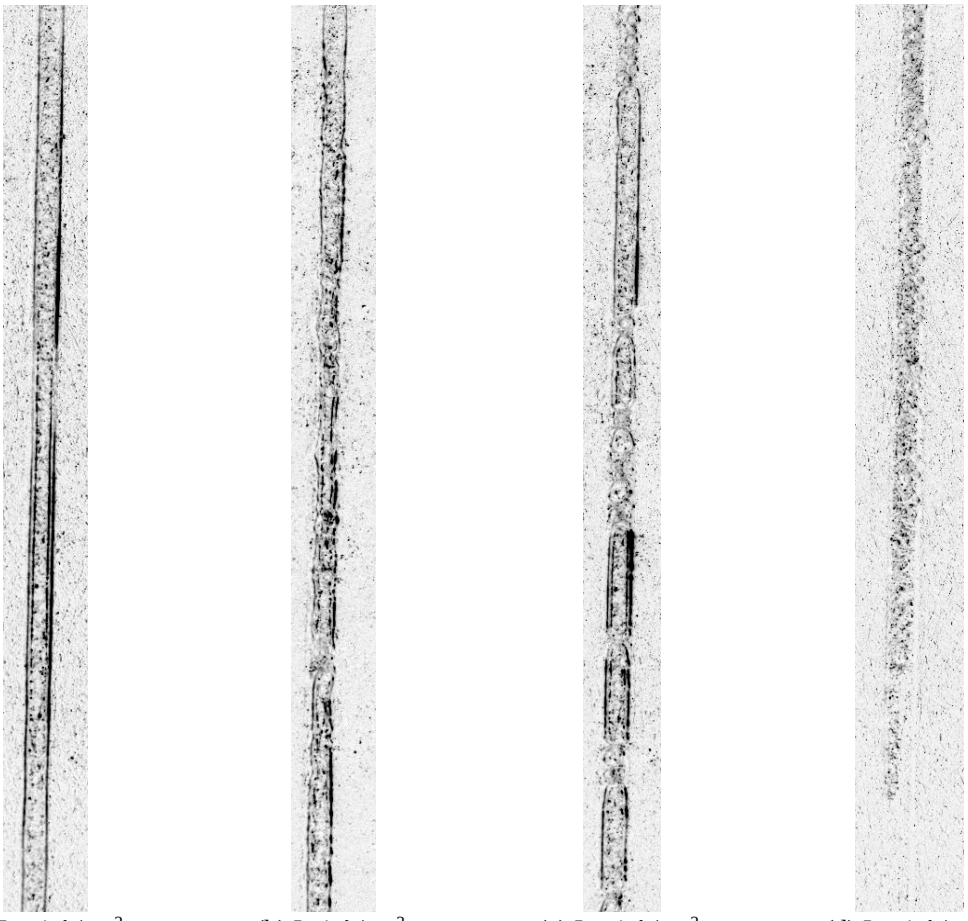

(a) I = 4 A/cm^2, WST=25 (b) I=4 A/cm^2, WST=50 (c) I = 4 A/cm^2, WST=100 (d) I = 4 A/cm^2, WST=200

Figure 5: Gas-liquid flow in the middle section of the channel, at fixed gas flow rate equivalent to 4 A/cm^2 and water flow rates equivalent to water stoichiometries of (a) 25, (b) 50, (c) 100, and (d) 200.

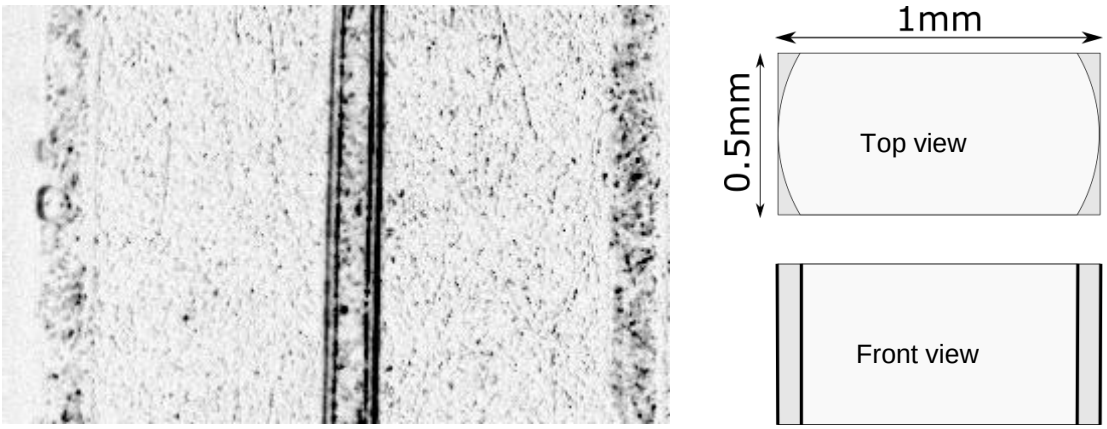

(a) (b)

Figure 6: Borders of annular bubble in the outgoing channel (a), bubble shape in the channel cross-section (top view) with the bubble (b). The large area of the channel, which gets dry in this flow condition and channel geometry.

Conclusion

In this work, different gas-liquid flow types in the micro-channel were studied, instead of studying an electrolysis cell, which is subject to complex electrochemical phenomena that affects the control of the test parameters. Along the channel length, breakup of annular and large Taylor bubbles by increasing water stoichiometry was observed. Since each of the gas-liquid flow regimes have their own specific heat transfer properties, the desired gas-liquid flow regime can be be obtained by setting the water stoichiometry. Meanwhile, it was seen at some point, the flow regime changed when changing the current density, even though the water stoichiometry was fixed because the superficial velocities are changing. By mapping the gas-liquid flow regimes for electrolyser micro-channels at several current densities and water stoichiometries, the gas-liquid regime could get controllable. It was seen that due to the rectangular cross sectional area of the channel, Taylor and annular bubbles get in contact with the channel walls. This resulted in dry walls, which can affect heat transfer. Even though the micro-porous ceramic plate gives a relatively uniform flow of air through the complete active surface area, the water pressure difference from inlet to the outlet of the channel affects it and we cannot guarantee a uniform bubble flow in the test section.

Acknowledgement

The authors acknowledge the funding provided by Innovation Fund Denmark through the e-STORE project.

References

1. M. Carmo, D. L. Fritz, J. Mergel, and D. Stolten, *Int. J. Hydrogen Energy*, **38**, 4901–4934 (2013).
2. M. Steilen and L. Jörissen, in *Electrochemical Energy Storage for Renewable Sources and Grid Balancing*,, p. 143–158, Elsevier (2014).
3. R. M. Krzysztof Lewinskia, Fuxia Suna, Sean Luopaa, Jiyoung Parka, in *1st International Conference on Electrolysis*,, Copenhagen (2017).
4. F. Fouda-Onana et al., *Int. J. Hydrogen Energy*, **41**, 16627–16636 (2016).
5. H. Ito, T. Maeda, A. Nakano, A. Kato, and T. Yoshida, *Electrochim. Acta*, **100**, 242–248 (2013).
6. J. Nie, Y. Chen, S. Cohen, B. D. Carter, and R. F. Boehm, *Int. J. Therm. Sci.*, **48**, 1914–1922 (2009).
7. H. Yang and T. S. Zhao, *Electrochim. Acta*, **50**, 3243–3252 (2005).
8. T. S. Zhao, C. Xu, R. Chen, and W. W. Yang, *Prog. Energy Combust. Sci.*, **35**, 275–292 (2009).
9. D. L. Wood, J. S. Yi, and T. V Nguyen, *Electrochim. Acta*, **43**, 3795–3809 (1998).
10. A. C. Olesen, C. Rømer, and S. K. Kær, *Int. J. Hydrogen Energy* (2015) .
11. S. S. Lafmejani, A. C. Olesen, and S. K. Kær, *Int. J. Hydrogen Energy*, 15 (2017).
12. O. F. Selamet et al., *Int. J. Hydrogen Energy*, **38**, 5823–5835 (2013).
13. I. Dedigama et al., *Int. J. Hydrogen Energy*, **39**, 4468–4482 (2014).
14. I. Dedigama et al., *J. Power Sources*, **265**, 97–103 (2014).
15. H. Yang, T. S. Zhao, and P. Cheng, *Int. J. Heat Mass Transf.*, **47**, 5725–5739 (2004).
16. S. Sadeghi Lafmejani, A. C. Olesen, and S. K. Kaer, *ECS Trans.*, **75**, 1121–1127 (2016).